遼寧師範大學
Liaoning Normal University

物理与电子技术学院
School of Physics and Electronic Technology, LNNU

CTEHEP-LNNU

Axion-like particles at future electron-positron colliders

Shuo Yang (杨硕)

(Liaoning Normal University)

based on

H.-Y. Zhang,C.-X. Yue, Y.-C. Guo and **SY**, PRD 104 (2021) 9, 096008.
C.-X. Yue, **SY**, H. Wang and N. Zhang, PRD 105(2022)11,115027.
SY, S.-Y. Song, S.-L. Zhang, C.-X. Yue, arXiv 2402.××××.

27th Mini-workshop on the frontier of LHC 2024-01-20

Outline

1. Introduction to axion-like particles (ALPs).
2. ALPs searches at colliders.
3. Searching for ALPs at future e^+e^- colliders
4. Conclusion

1.Introduction to axion-like particles

- The discovery of Higgs bring us into a new territory of spin-0 particles.
- The axion has been postulated to address the strong CP problem,which is the pNGB associated to Peccei-Quinn symmetry, a global U(1).
- Many extensions of the SM feature one or several spontaneously broken global U(1) symmetries, thus predicting axion-like particles (ALPs).
- ALPs：There is no direct relation between couplings and mass which induce rich phenomena.

General effective Lagrangian of ALPs

bottom-up view

ALPs can be described in a EFT where heavy sector is integrated out

SMEFT $$\mathcal{L} = \mathcal{L}_0 + \sum_i \frac{c_i}{\Lambda^{d-4}} \mathbf{O}_i$$

Building Blocks：

SM fields： $B_{\mu\nu}, W_{\mu\nu}, G_{\mu\nu}$

EW scalar doublet: $\Phi(x) = \frac{v + h(x)}{\sqrt{2}} e^{i\vec{\pi}\vec{\sigma}/v}$

New pseduscalar (GB): $\frac{\partial_\mu a}{f_a}$

General effective Lagrangian of ALPs

Linear Effective Lagrangian

NLO bosonic operators

$$\mathbf{O}_{\tilde{B}} = -B_{\mu\nu}\tilde{B}^{\mu\nu}\frac{a}{f_a} \qquad \mathbf{O}_{\tilde{G}} = -G^a_{\mu\nu}\tilde{G}^{a\mu\nu}\frac{a}{f_a}$$

$$\mathbf{O}_{\tilde{W}} = -W_{\mu\nu}\tilde{W}^{\mu\nu}\frac{a}{f_a} \qquad \mathbf{O}_{a\Phi} = i(\Phi^\dagger \overleftrightarrow{D}_\mu \Phi)\frac{\partial^\mu a}{f_a}$$

$$\mathcal{L}_{\rm eff}^{D\le 5} = \frac{1}{2}(\partial_\mu a)(\partial^\mu a) - \frac{M_a^2}{2}a^2 + \frac{\partial^\mu a}{\Lambda}\sum_F \bar{\psi}_F C_F \gamma_\mu \psi_F$$
$$+ g_s^2 C_{GG}\frac{a}{\Lambda}G^A_{\mu\nu}\tilde{G}^{\mu\nu,A} + g^2 C_{WW}\frac{a}{\Lambda}W^A_{\mu\nu}\tilde{W}^{\mu\nu,A} + g'^2 C_{BB}\frac{a}{\Lambda}B_{\mu\nu}\tilde{B}^{\mu\nu}$$

$$\mathcal{L}_{\rm eff}^{D\ge 6} = \frac{c_{ah}}{f^2}(\partial_\mu a)(\partial^\mu a)\,\phi^\dagger\phi + \frac{c_{Zh}}{f^3}(\partial^\mu a)\left(\phi^\dagger\, iD_\mu\,\phi + \text{h.c.}\right)\phi^\dagger\phi + \ldots$$

H.Georgi,D.B.Kaplan& L.Randall, PLB169(1986)73-78

M.Bauer et al., JHEP12(2017),044

I.Brivio et al., EPJC77(2017),8,572 (including Noliner Effective Lagrangian)

2. ALPs searches at colliders

Prodcution modes

- Resonant production

$gg \to a \quad \gamma\gamma \to a$

$e^+e^- \to a$ strongly suppresed

- Associated production

$pp \to a\,W^\pm \quad pp \to aZ(\gamma)$

$pp \to a\,h \quad pp \to t\,\bar{t}\,a \quad pp \to aW^\pm\gamma$

$e^+e^- \to aZ(\gamma) \quad e^+e^- \to ah$

$e^+e^- \to e^+e^-a \quad e^+e^- \to \nu\bar{\nu}a$

- Exotic SM decays

$h \to Za \quad h \to aa \quad Z \to a\gamma$

- Meson decays
- Other modes

Decay channels

- Stable ALPs ~ $\not{E}$

- Long-Lived ALPs with a Displaced-Vertex

- Short lived ALP

$a \to \gamma\gamma \quad a \to \ell^+\ell^- \quad a \to jj$

$a \to b\bar{b} \quad a \to VV \quad a \to t\bar{t}$

I.Brivio et al., EPJC77(2017),8,572
M.Bauer et al., EPJC79(2019),1,74
CERN Yellow Rep. Monogr. Vol. 3 (2018)

3.Searching for ALPs at future e+e- colliders

3.1 Light-by-light scattering

H-Y Zhang，C-X Yue, Y-C Guo and ***SY,*** PRD 104 (2021) 9, 096008

- The LHC generally is more sensitive to the heavy ALP searches by LBL scattering. The CLIC studies obtain a stonger bounds for TeV ALPs.

C.Baldenegro et al., JHEP06,(2018)131 (LHC LBL)
S.C. Inan and A.V. Kisselev, JHEP06(2020)183;
Chin.Phys.C 45 (2021) 4, 043109 (CLIC LBL)

- It is interesting to study LBL at the CEPC and FCC-ee.

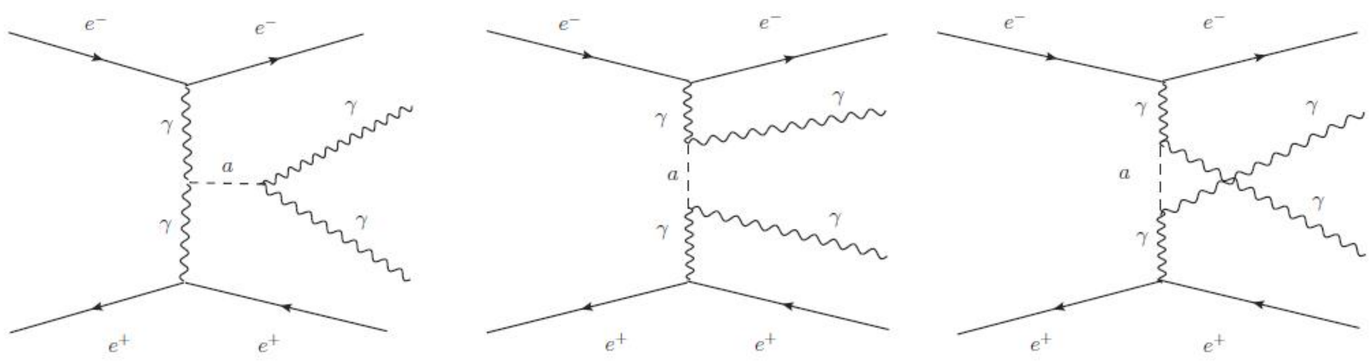

3.1 Light-by-light scattering

Cross sections for light-by-light scattering process

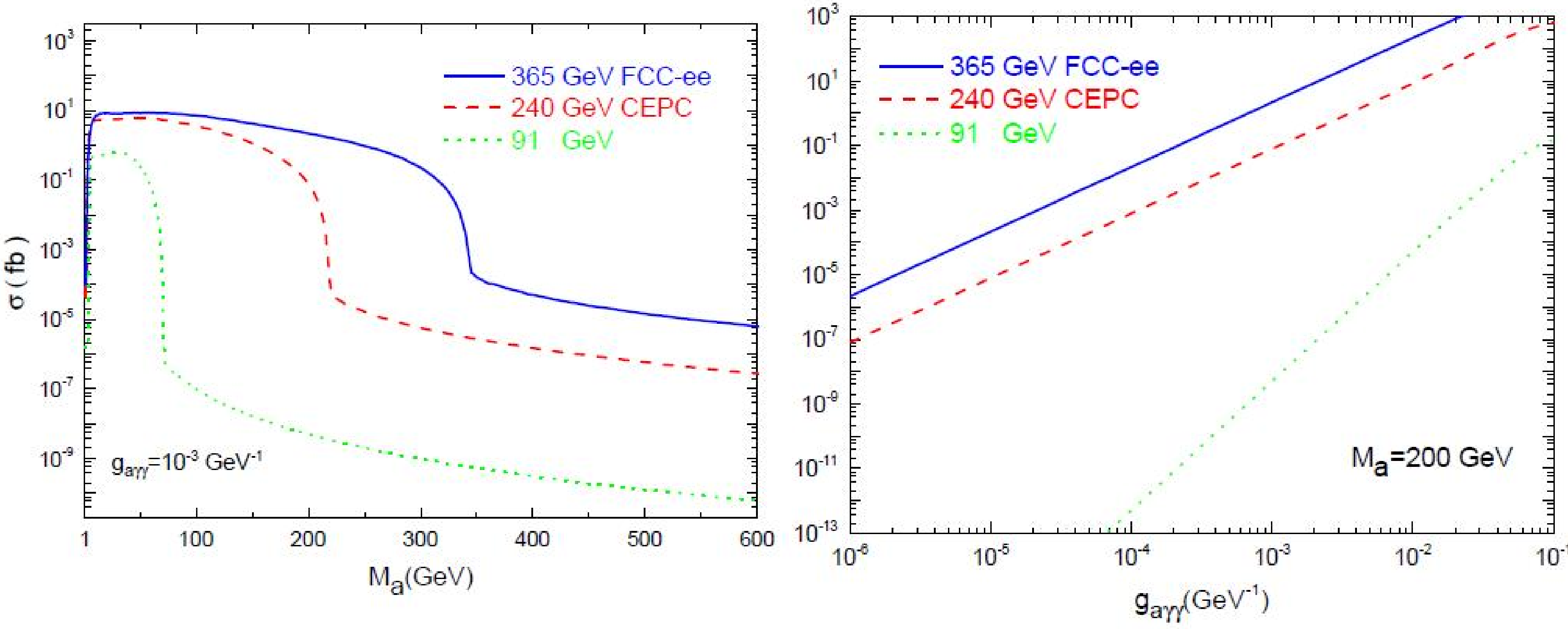

(a) (b)

3.1 Light-by-light scattering

Backgound for the LBL signal

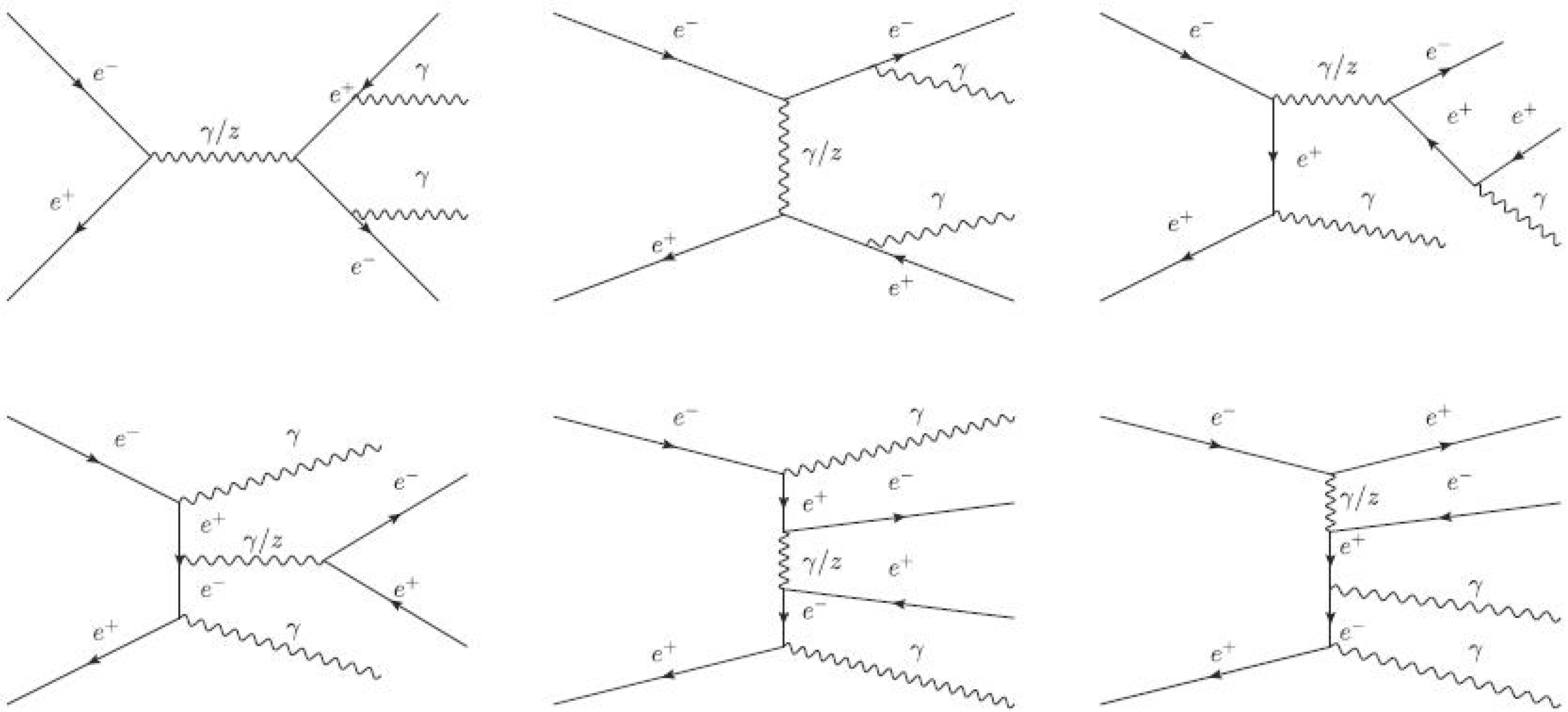

FIG. 3. The typical diagrams for the background of the process $e^+e^- \to \gamma\gamma e^+e^-$.

3.1 Light-by-light scattering

Detecting ALPs at the CEPC

Cuts	$\sqrt{s} = 240$ GeV	$\sqrt{s} = 91$ GeV
Cut-1: Electron and positron pseudo-rapidity	$0.4 < \eta(e^+) < 2.4$ $-2.4 < \eta(e^-) < -0.4$	$-0.3 < \eta(e^+) < 0.9$ $-0.9 < \eta(e^-) < 0.3$
Cut-2: Angle between the ALP and the beam axis	$0.7 < \theta(\gamma\gamma) < 2.4$	$0.7 < \theta(\gamma\gamma) < 2.4$
Cut-3: Angular separation between electron-positron	$\Delta\theta(e^+e^-) < 2.9$	$\Delta\theta(e^+e^-) < 2.4$
Cut-4: Transverse momentum of reconstructed diphotons	$p_T(\gamma\gamma) > 45$ GeV	$p_T(\gamma\gamma) > 20$ GeV

CEPC @ $\sqrt{s} = 240$ (91) GeV							
Cuts	Signal (fb)						Background (fb)
	$M_a = 6$ GeV	$M_a = 8$ GeV	$M_a = 10$ GeV	$M_a = 50$ GeV	$M_a = 100$ GeV	$M_a = 160$ GeV	$\gamma\gamma e^+e^-$
Basic cuts	3.4378(0.249)	4.8088(0.4796)	5.2928(0.5003)	5.9064(0.2432)	3.585	0.8021	67.0614(98.8986)
Cut 1	2.9865(0.0316)	3.932(0.1267)	4.138(0.1417)	4.5336(0.0977)	2.4778	0.4436	33.7026(40.928)
Cut 2	2.1714(0.0309)	3.0176(0.1264)	3.2819(0.1411)	3.1262(0.0904)	1.6993	0.3145	12.628(34.93)
Cut 3	2.1368(0.0226)	3.0383(0.1156)	3.2422(0.1297)	3.0238(0.0717)	1.6497	0.3052	9.042(8.396)
Cut 4	1.4(0.0226)	2.2984(0.1156)	2.5065(0.1297)	2.0519(0.0501)	0.8747	0.0392	3.3614(6.1921)

3.1 Light-by-light scattering

Prospects for detecting ALP at CEPC

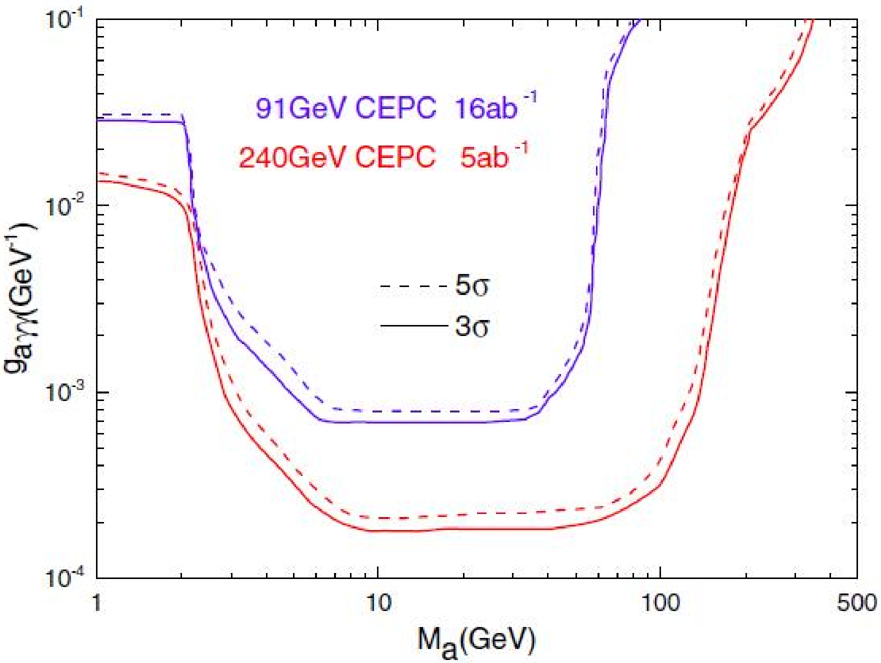

The 3σ and 5σ discovery curves in the $M_a - g_{a\gamma\gamma}$ plane at the CEPC.

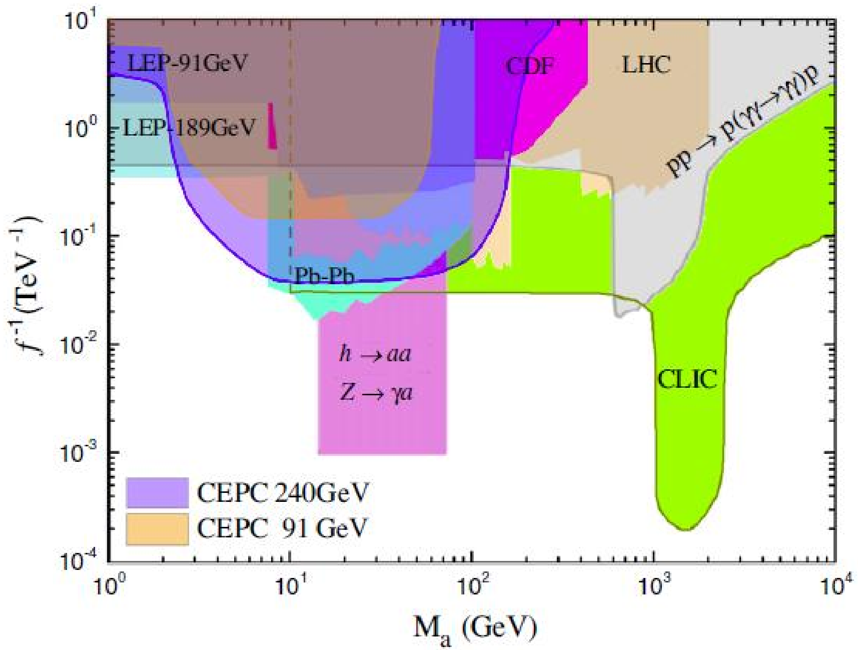

The 95% C.L exclusion regions in the $M_a - g_{a\gamma\gamma}$ plane at the CEPC and other colliders

$\sqrt{s} = 91$ GeV, $\mathcal{L} = 16$ ab^{-1} $\quad$ $\sqrt{s} = 240$ GeV, $\mathcal{L} = 5.0$ ab^{-1}

3.1 Light-by-light scattering

ALPs at the CEPC & FCC-ee

CEPC @ $\sqrt{s} = 240$ (91) GeV							
Cuts	Signal (fb)						Background (fb)
	M_a = 6 GeV	M_a = 8 GeV	M_a = 10 GeV	M_a = 50 GeV	M_a = 100 GeV	M_a = 160 GeV	$\gamma\gamma e^+e^-$
Basic cuts	3.4378(0.249)	4.8088(0.4796)	5.2928(0.5003)	5.9064(0.2432)	3.585	0.8021	67.0614(98.8986)
Cut 1	2.9865(0.0316)	3.932(0.1267)	4.138(0.1417)	4.5336(0.0977)	2.4778	0.4436	33.7026(40.928)
Cut 2	2.1714(0.0309)	3.0176(0.1264)	3.2819(0.1411)	3.1262(0.0904)	1.6993	0.3145	12.628(34.93)
Cut 3	2.1368(0.0226)	3.0383(0.1156)	3.2422(0.1297)	3.0238(0.0717)	1.6497	0.3052	9.042(8.396)
Cut 4	1.4(0.0226)	2.2984(0.1156)	2.5065(0.1297)	2.0519(0.0501)	0.8747	0.0392	3.3614(6.1921)

FCC-ee @ $\sqrt{s} = 365$ (91) GeV							
Cuts	Signal (fb)						Background (fb)
	M_a = 6 GeV	M_a = 8 GeV	M_a= 10 GeV	M_a= 50 GeV	M_a= 100 GeV	M_a= 200 GeV	$\gamma\gamma e^+e^-$
Basic cuts	2.9092(0.2483)	5.0074(0.4786)	6.5272(0.5001)	8.4206(0.2432)	7.1235	2.1737	54.203(98.8188)
Cut 1	2.1634(0.0311)	4.2978(0.1265)	5.3419(0.142)	4.5123(0.0977)	4.9093	1.2593	29.233(41.0505)
Cut 2	1.3962(0.0307)	2.6956(0.1261)	3.6755(0.1416)	2.9963(0.0904)	3.1011	0.7942	8.3373(35.0206)
Cut 3	1.2374(0.0223)	2.5417(0.1152)	3.5173(0.1304)	2.8482 (0.0717)	2.9926	0.768	4.8137(8.4019)
Cut 4	0.9014(0.0222)	2.2243(0.115)	3.1819(0.1303)	2.5198(0.05)	2.5458	0.453	2.6445(6.1842)

3.2 Exotic decay $Z \to af\bar{f}$ at future Z factories

C.-X. Yue, **SY**, H. Wang and N. Zhang, PRD 105(2022)11,115027

- CEPC and FCC-ee can produce up to 10^{12} Z bosons.
- It is possible for the observations of rare decays of Z.
- We foucus on four types of exotic Z-decay signals

$Z \to \mu^+\mu^-\not{E}, b b\not{E}, e^+e^-\mu^+\mu^-$ and e^+e^-bb .

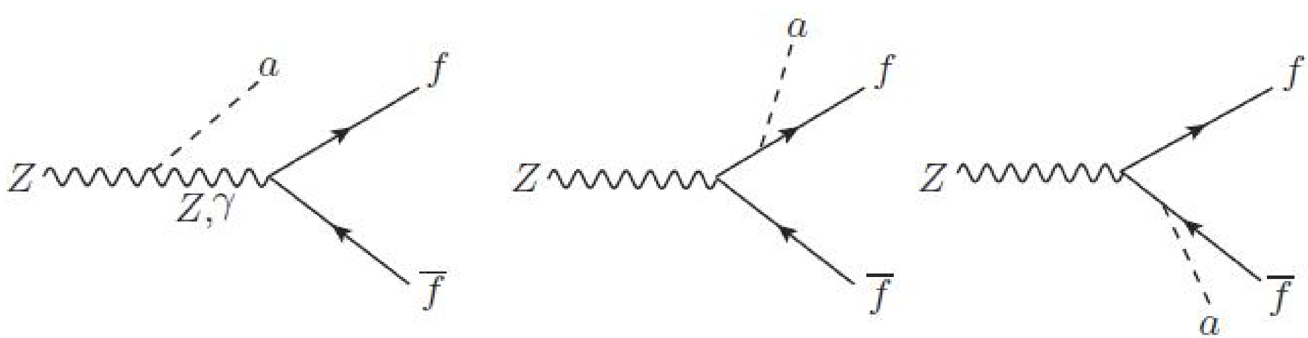

3.2 Exotic decay $Z \to af\bar{f}$ at future Z factories

$Z \to \mu^+\mu^-\not{E}$ and $Z \to bb\not{E}$

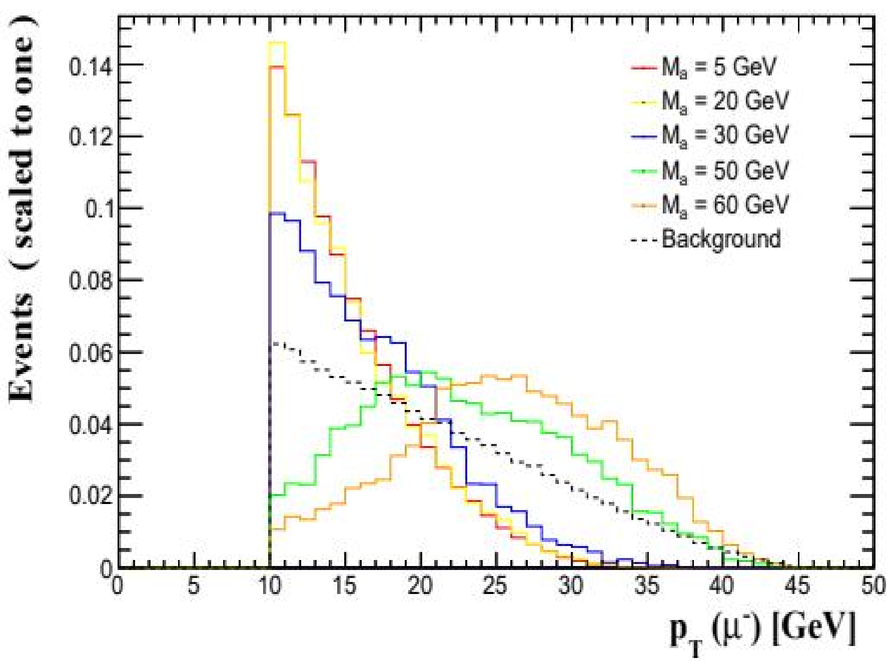

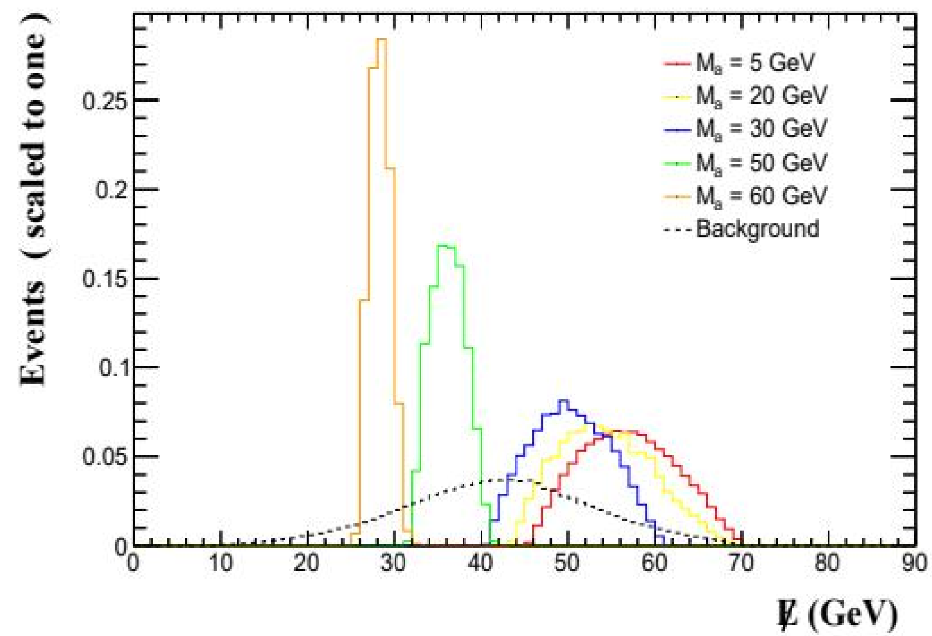

The normalized distribution for kinematic variables for signal $\mu^+\mu^-\not{E}$ and BG.

3.2 exotic decay $Z \to af\bar{f}$ at future Z factories

$Z \to \mu^+\mu^- \not{E}$ and $Z \to bb\not{E}$

$P_T(l,j) > 10\text{GeV},\ \not{E} > 10\text{GeV},\ |\eta(l,j)| < 2.5,\ \theta_{ij}(l,l) > 0.2,\ \theta_{ij}(j,j) > 0.4,$

Cuts	Cross sections for signal(background) (fb)				
	m_a = 5GeV	m_a = 10GeV	m_a = 30GeV	m_a= 50GeV	m_a= 60GeV
Basic cuts	0.3406(0.2602)	0.3177(0.2602)	0.2368(0.2602)	0.0358(0.2602)	0.0062(0.2602)
Cut 1-A	0.3404(0.0059)	0.3175(0.0072)	0.2335(0.0300)	0.0343(0.0342)	0.0058(0.0195)
$S/\sqrt{S+B}$	18.29	17.62	14.38	5.59	1.16

Cut1-A

$|m_{\mu^+\mu^-} - m_a| < 3$ GeV

Cuts	Cross sections for signal(background) (fb)				
	m_a = 15GeV	m_a = 30GeV	m_a= 40GeV	m_a= 50GeV	m_a=60GeV
Basic cuts	0.0460(0.7172)	0.03345(0.7172)	0.0284(0.7172)	0.0142(0.7172)	0.0134(0.7172)
Cut 1-B	0.0449(0.0126)	0.0279(0.08387)	0.0199(0.1832)	0.0078(0.2115)	0.0015(0.1364)
$S/\sqrt{S+B}$	5.92	2.64	1.39	0.53	0.12

Cut1-B

$|m_{bb} - m_a| < 5$ GeV

For an integrated luminosity of 1 ab^{-1}.

$Z \to e^+e^-\mu^+\mu^-$ and $Z \to e^+e^-bb$

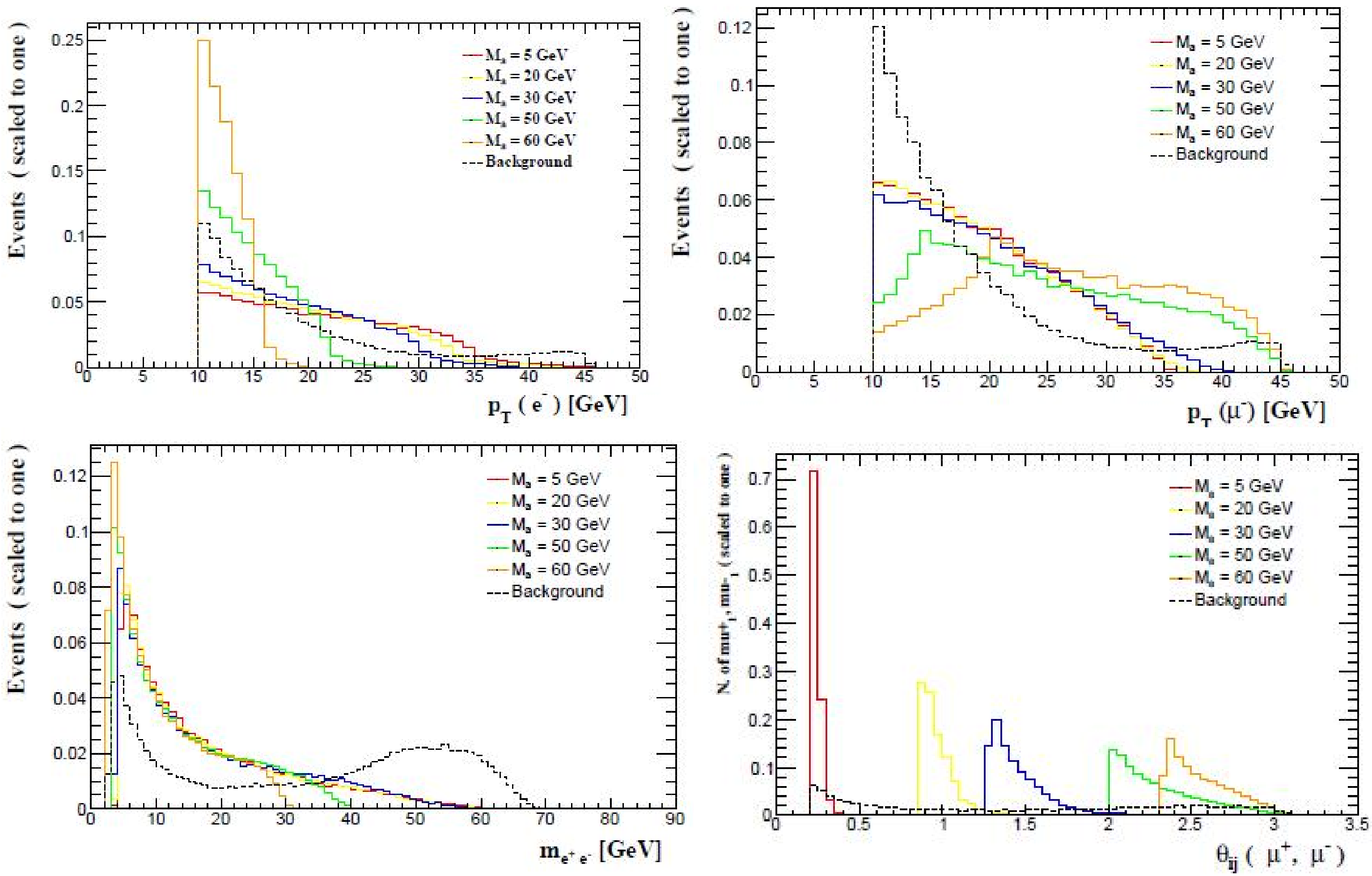

The normalized distribution for kinematic variables for signal $e^+e^-\mu^+\mu^-$ and BG.

$Z \to e^+e^-\mu^+\mu^-$ and $Z \to e^+e^-bb$

Cuts	Cross sections for signal(background) (fb)				
	m_a = 5GeV	m_a = 10GeV	m_a= 30GeV	m_a= 50GeV	m_a= 60GeV
Basic cuts	1.5314(8.0284)	1.4735(8.0284)	1.1559(8.0284)	0.4615(8.0284)	0.1067(8.0284)
Cut 1-C	1.2659(3.4300)	1.2231(3.4300)	0.9318(3.4300)	0.4258(3.4300)	0.1065(3.4300)
Cut 2-C	1.2659(0.1743)	1.2215(0.1623)	0.9143(0.1689)	0.4066(0.6499)	0.1005(0.5635)
$S/\sqrt{S+B}$	33.36	32.83	27.78	12.51	3.90

Cut-C

$m_{e^+e^-} < 30$ GeV

$|m_{\mu^+\mu^-} - m_a| < 3$ GeV

Cuts	Cross sections for signal(background) (fb)				
	m_a = 15GeV	m_a = 30GeV	m_a= 40GeV	m_a= 50GeV	m_a= 60GeV
Basic cuts	0.2058(2.7076)	0.2497(2.7076)	0.1874(2.7076)	0.1191(2.7076)	0.0354(2.7076)
Cut 1-D	0.1711(1.8332)	0.2251(1.8332)	0.1658(1.8332)	0.1103(1.8332)	0.0353(1.8332)
Cut 2-D	0.1694(0.1417)	0.1763(0.2081)	0.1106(0.3301)	0.0617(0.5102)	0.0160(0.4212)
$S/\sqrt{S+B}$	9.61	8.99	5.27	2.58	0.76

Cut-D

$m_{e^+e^-} < 30$ GeV

$|m_{bb} - m_a| < 5$ GeV

For an integrated luminosity of 1 ab^{-1}.

3.2 Exotic decay $Z \to a f\bar{f}$ at future Z factories

Sensitivity bounds

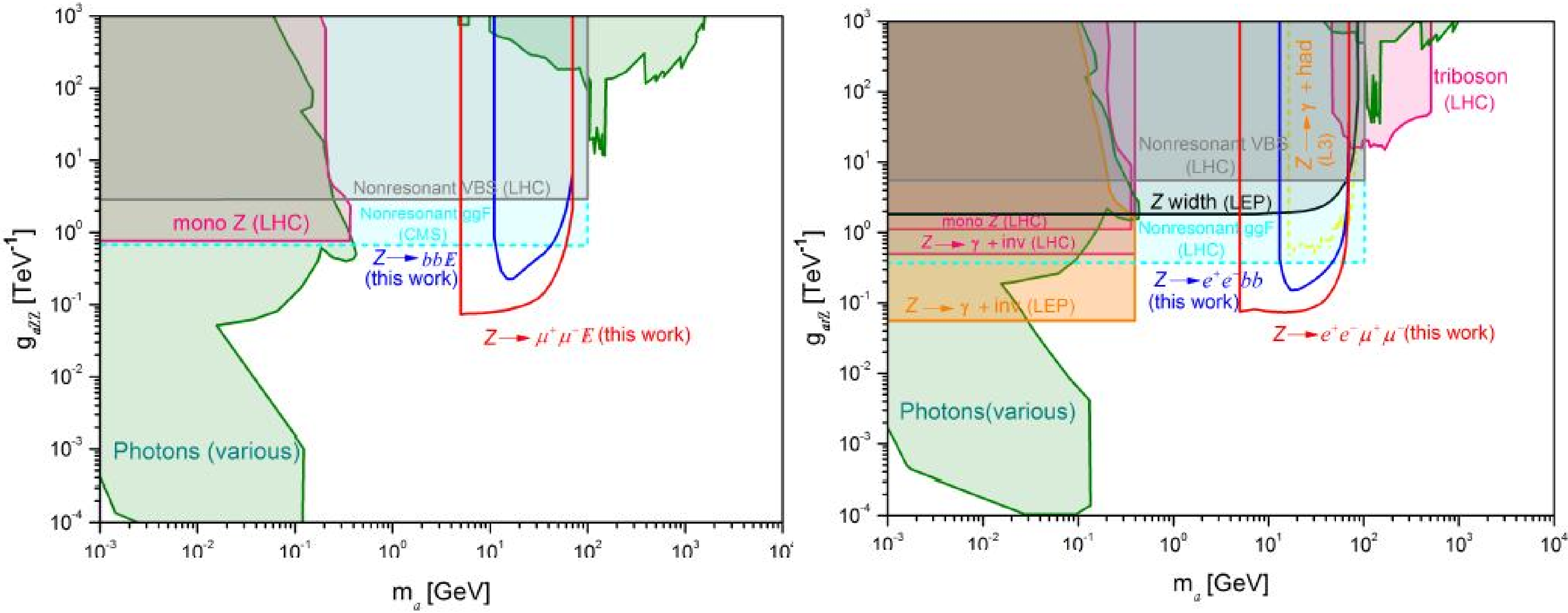

Sensitivity bounds on g_{aZZ} and $g_{a\gamma Z}$ at 95% C.L. from exotic Z decays and other current exclusion regions.

3.3 Fully hadronic channel for heavy ALPs at CLIC

- High energy lepton colliders with clean evironments can provide new and complementary discovery potential to the LHC.
- The high collision energy and high-luminosity of future CLIC make it possible to test the ALPs in a larger mass range.
- A heavy ALP in fully hadronic channel will result in highly boosted jets.

ALPs in fully hadronic channel at CLIC

SY, S.-Y. Song, S.-L. Zhang, C.-X. Yue, arXiv 2402.××××.

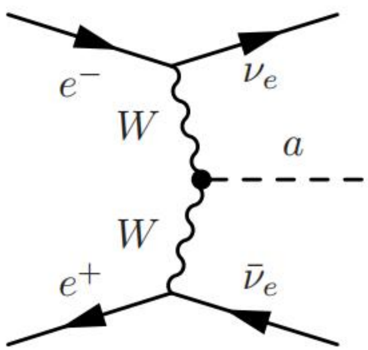

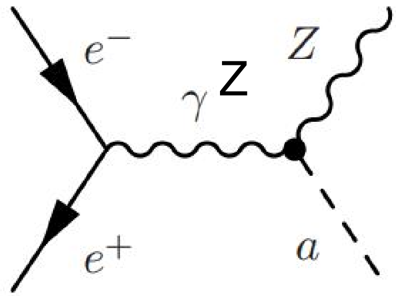

Signal : $e^+e^- \to a\nu\bar{\nu} \to WW\nu\bar{\nu} \to jets + \not{E}$

Valencia jet algorithm is taken.

Backgrounds includes WWZ、WW、tt、jjvv.

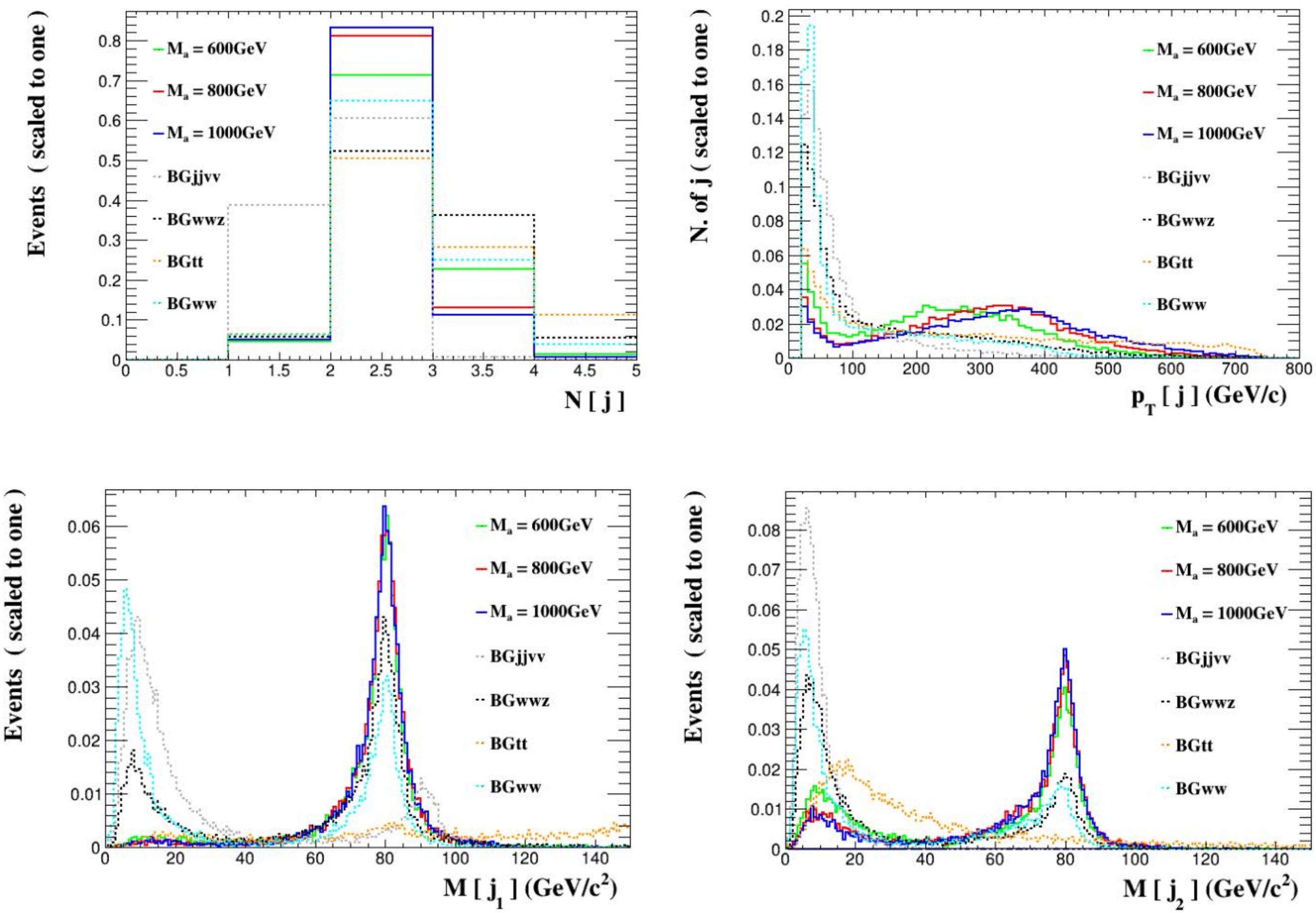

The normalized distribution for kinematic variables for the signal and BG.

Imporved cuts

1. Cut1: the number of jets in the final state satisfies $N(j) > 1$ and $N(l) = 0$.
2. Cut2: the mass of j_1 is in the range of $70\ \text{GeV} < m_{j_1} < 90\ \text{GeV}$.
3. Cut3: the mass of j_2 is required to $70\ \text{GeV} < m_{j_2} < 90\ \text{GeV}$ or $70\ \text{GeV} < m_{j_2} m_{j_3} < 90\ \text{GeV}$.
4. Cut4: missing transverse momentum $\not{E}_T$ satisfies $\not{E}_T > 100\ \text{GeV}$.
5. Cut5: the number of bottom quark $N(b) < 2$.

3.3 Fully hadronic channel for heavy ALPs at CLIC

Cross sections for signal and background(fb)							
Cuts	$m_a = 600$ GeV	$m_a = 800$ GeV	$m_a = 1000$ GeV	BGWWZ	BGWW	BG$t\bar{t}$	BG$jj\nu\nu$
Basic cut	2.9168	1.392	0.442	1.9106	227.803	6.2827	561.534
Cut1	2.670	1.2789	0.4076	1.6667	201.099	0.3929	340.018
Cut2	2.0361	1.0089	0.3206	0.9082	77.990	0.0315	0.2374
Cut3	1.4658	0.7082	0.2289	0.5610	47.765	0.00315	0
Cut4	1.3832	0.646	0.2072	0.4307	0.3491	0.00252	0
Cut5	1.3525	0.628	0.2007	0.4147	0.3491	0.0006	0
$S/\sqrt{S+B}$	29.396	16.829	6.46				

CLIC@1.5TeV for an integrated luminosity of 1 ab^{-1}.

Cross sections for signal and background(fb)							
Cuts	$m_a = 800$ GeV	$m_a = 1000$ GeV	$m_a = 1500$ GeV	BGWWZ	BGWW	BG$t\bar{t}$	BG$jj\nu\nu$
Basic cut	3.911	2.206	0.4678	0.7168	32.118	0.8422	851.925
Cut1	3.6099	2.0235	0.4263	0.578	28.549	0.0798	460.645
Cut2	2.819	1.5754	0.333	0.3104	15.751	0.00296	0.9399
Cut3	1.9714	1.0842	0.2194	0.1465	7.4188	0.000422	0
Cut4	1.8487	1.0222	0.2078	0.1156	0.05274	0	0
Cut5	1.8008	0.9917	0.1992	0.1101	0.04395	0	0
$S/\sqrt{S+B}$	40.72	29.688	10.597				

CLIC@3.0TeV for an integrated luminosity of 1 ab^{-1}.

work in progress

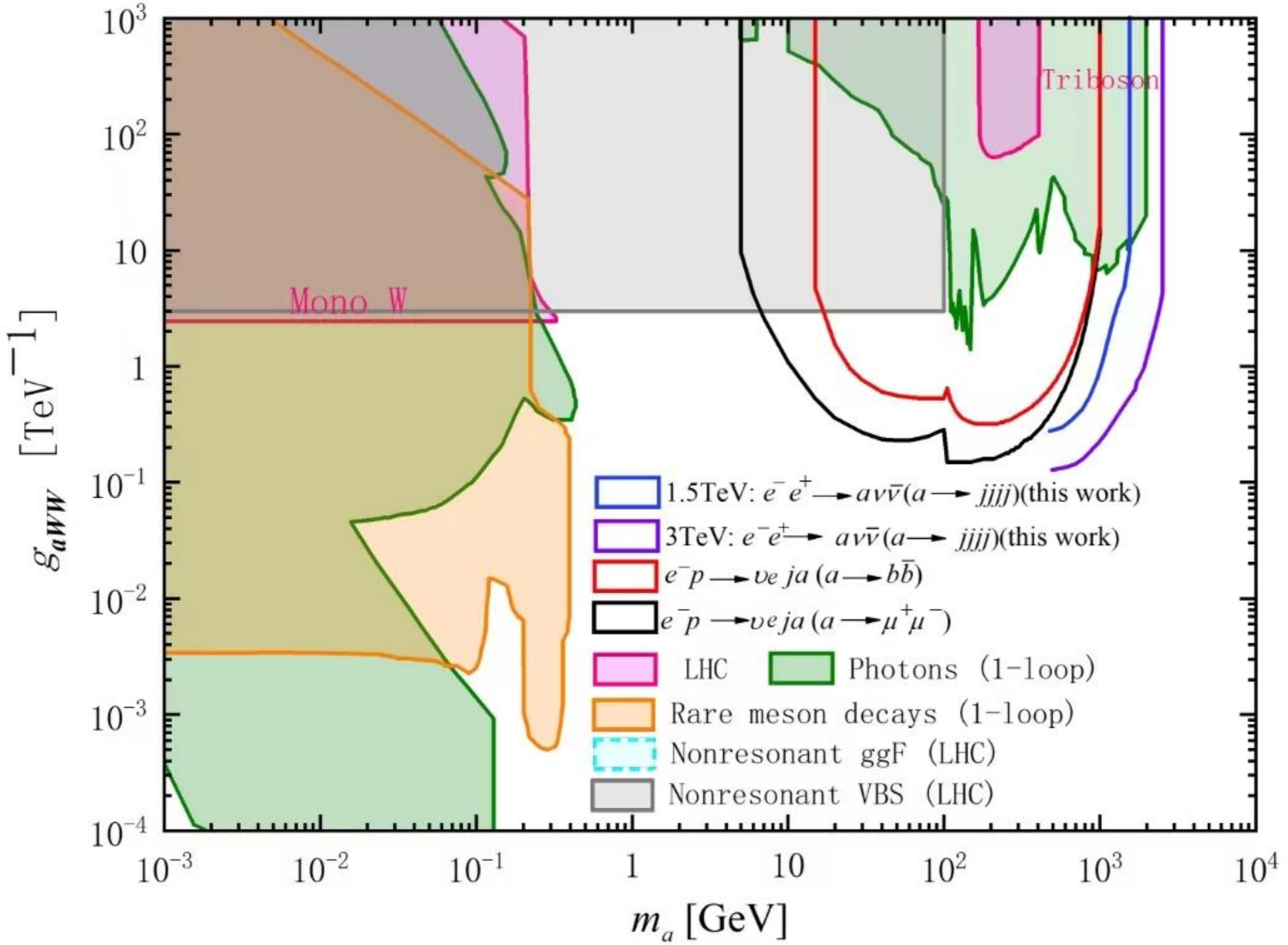

Sensitivity bounds on g_{aWW} at 95% C.L. and other current exclusion regions.

Conclusion

- ALPs have a much wider parameter space and hence generate rich phenomenology at colliders.
- Future electron-positron colliders can provide a good environment to exploring ALPs.
- Several interesting searching channels for ALPs are consiered(LBL， Z->aff, avv->jets+missing energy), it is expected that the future e^+e^- colliders could discover or exclude ALPs.


Thank You!

Backup

Vertices

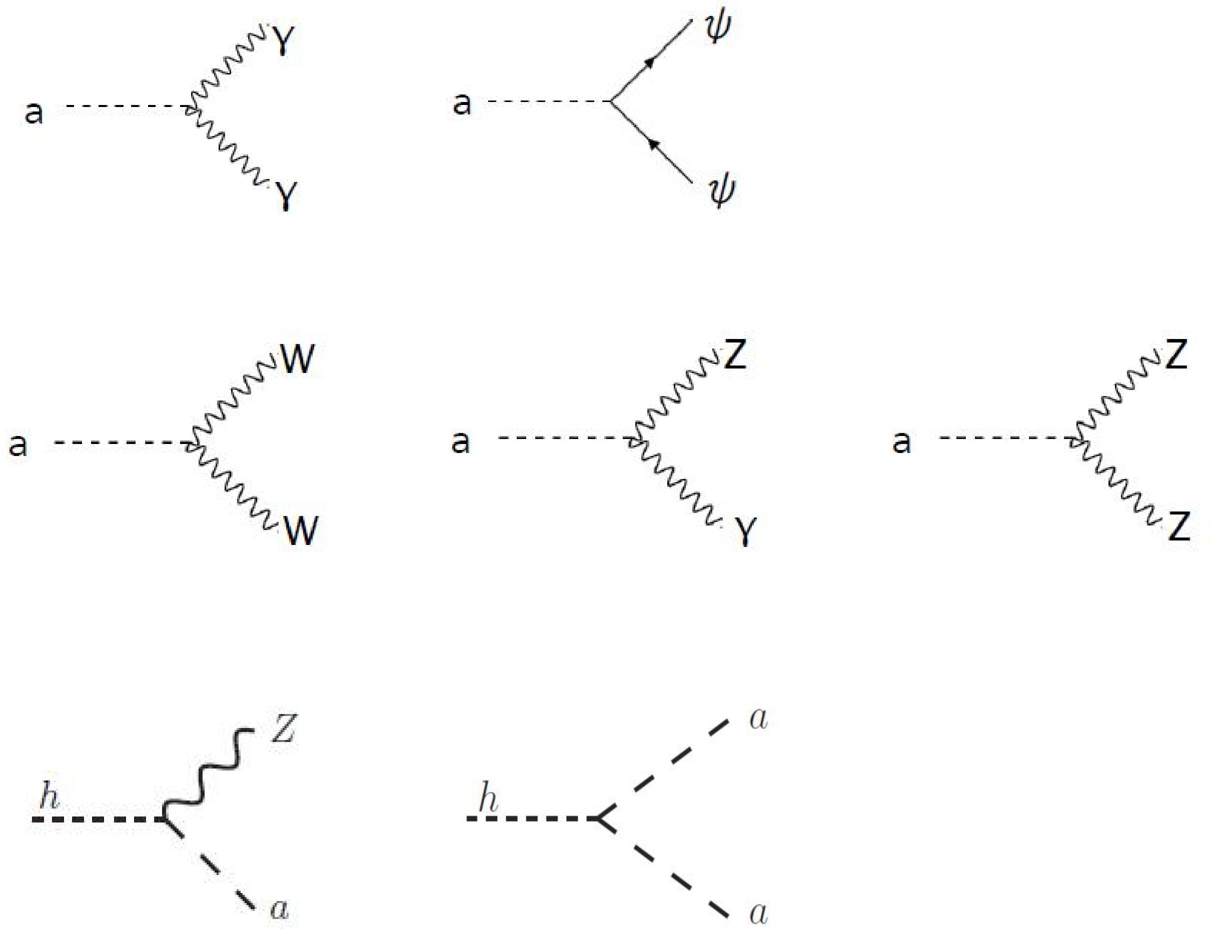

Distrubtions of kinematic variables

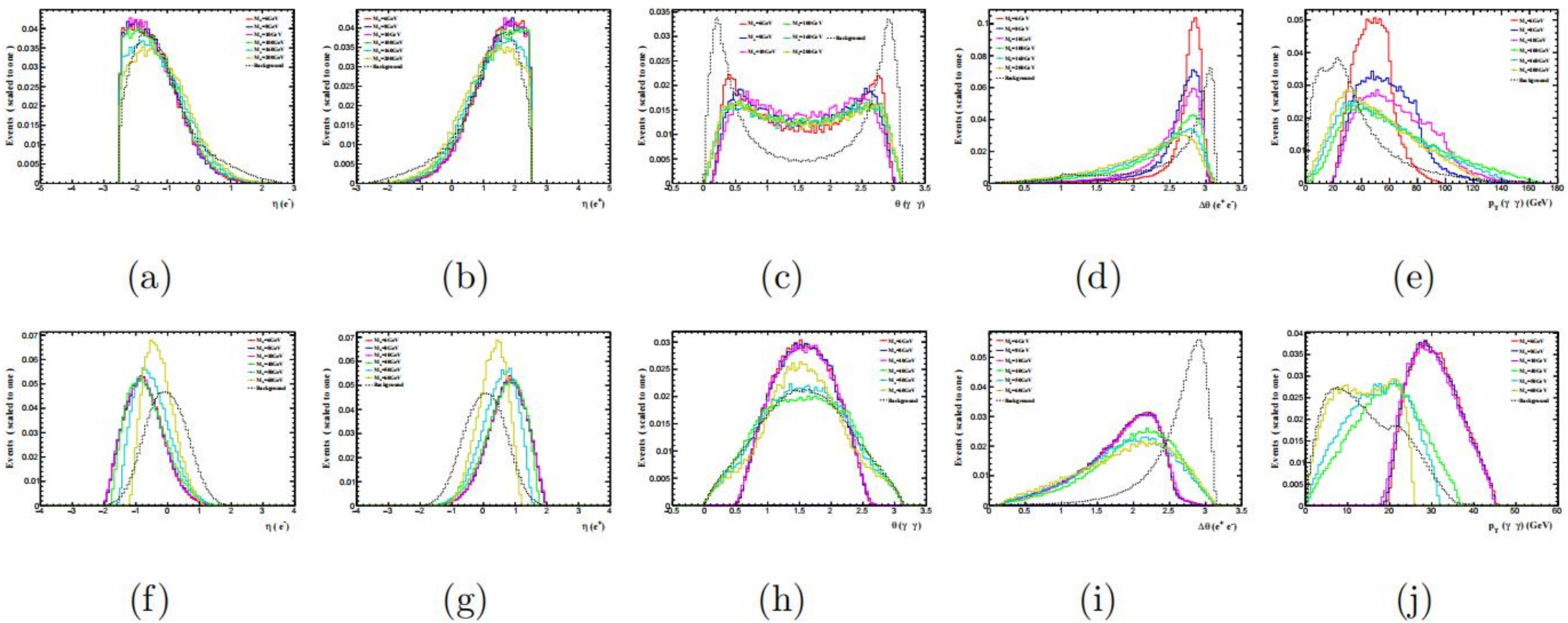

FIG. 4: Normalized distributions of $\eta(e^{\pm})$, $\theta(\gamma\gamma)$, $\Delta\theta(e^{+}e^{-})$, $p_T(\gamma\gamma)$ for the signal of selected ALP masses and background at 365 GeV (a, b, c, d, e) and 91 GeV (f, g, h, i, j) FCC-ee with designed luminosities.

Prospects for detecting ALP at CEPC

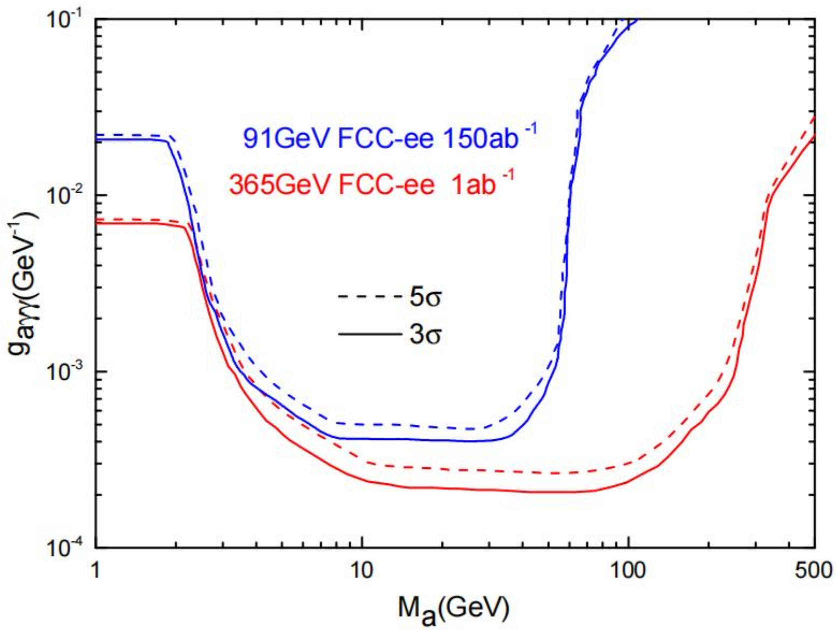

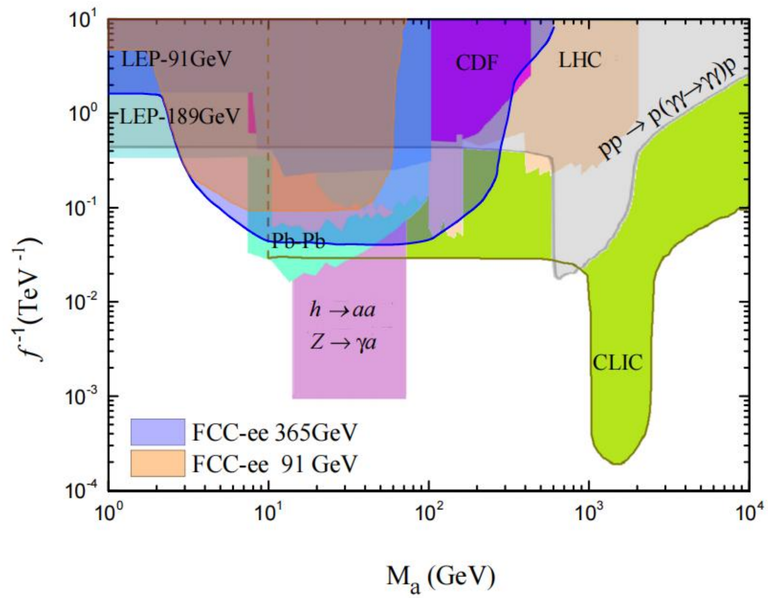

jet clustering alogrithm	d_{ij}	d_{iB}
VLC	$2\min(E_i^{2\beta},\ E_j^{2\beta})\frac{1-cos\theta_{ij}}{R^2}$	$E_i^{2\beta}sin^{2\gamma}\theta_{iB}$
$generalized\ e^+e^-$	$2\min(E_i^{2n},\ E_j^{2n})\frac{1-cos\theta_{ij}}{1-cosR}$	E_i^{2n}
k_t	$\min(P_{Ti}^2,\ P_{Tj}^2)\frac{\Delta R_{ij}^2}{R^2}$	P_{Ti}^2
CA	$\frac{\Delta R_{ij}^2}{R^2}$	1
Aiti-k_t	$\min(P_{Ti}^{-2},\ P_{Tj}^{-2})\frac{\Delta R_{ij}^2}{R^2}$	P_{Ti}^{-2}